Quantum image filtering and its reversible logic circuit design

Gaofeng Luo

College of Information Engineering,
Shaoyang University,
Shaoyang, China
Email: gfluo12@163.com

Shexiang Jiang*

School of Computer Science and Engineering,
Anhui University of Science and Engineering,
Huaunan, 232001, China
Email: sxjiang8888@163.com
*Corresponding author

Liang Zong

College of Information Engineering,
Shaoyang University,
Shaoyang, China
Email: kevzong@qq.com

Abstract: Quantum information processing can overcome the limitations of classical computation. Consequently, image filtering using quantum computation has become a research hotspot. Here, a quantum algorithm is presented on the basis of the classical image filtering principle to detect and cancel the noise of an image. To this end, a quantum algorithm that completes the image filtering task is proposed and implemented. The novel enhanced quantum representation of digital images is introduced. Then, four basic modules, namely, position-shifting, parallel-CNOT, parallel-swap, and compare the max, are demonstrated. Two composite modules that can be utilised to realise the reversible logic circuit of the proposed quantum algorithm are designed on the basis of these basic modules. Simulation-based experimental results show the feasibility and the capabilities of the proposed quantum image filtering scheme. In addition, our proposal has outperformed its classical counterpart and other existing quantum image filtering schemes supported by detailed theoretical analysis of the computational complexity. Thus, it can potentially be used for highly efficient image filtering in a quantum computer age.

Keywords: quantum computing; reversible logic circuit; image filtering.

Reference to this paper should be made as follows: Luo, G., Jiang, S. and Zong, L. (2021) 'Quantum image filtering and its reversible logic circuit design', *Int. J. Embedded Systems*, Vol. 14, No. 3, pp.248–258.

Biographical notes: Gaofeng Luo received his MS in Information and Communication Engineering from the Central South University, Changsha, China, in 2010, and PhD from Shanghai Maritime University, Shanghai, China, in 2020. He is an Associate Professor with the College of Information Engineering, Shaoyang University. His research interests include intelligent information processing and information security.

Shexiang Jiang is currently pursuing his PhD in Information System at the Shanghai Maritime University, Shanghai, China. He is a Lecturer with the School of Computer Science and Engineering, Anhui University of Science and Technology. His research interests include quantum image processing, quantum communication and quantum teleportation.

Liang Zong received his PhD from the Hainan University, Haikou, China, in 2016. He is a Lecturer with the College of Information Engineering, Shaoyang University. His research interests include embedded system and information security.

1 Introduction

Several researchers hope to exploit the distinct properties of quantum, (i.e., superposition and entanglement) as a novel computational model. Feynman (1982) was the first person to come up with this concept. In 1994, Shor proposed a quantum integer factorisation algorithm that could obtain the key encryption of RSA in polynomial time. In 1996, Grover published a special algorithm that could obtain quadratic speed theoretically for databased searching. Quantum computing is considered an important method for breaking the limitations of classical computing (Wang et al., 2017).

Following the image sensors' development, the number of images is increasing, especially for some real-time images (Wang and Vinter, 2016). A more efficient method is required to store and process large-scale images (Zhang et al., 2018). Thus, image processing in a quantum computer begins to emerge into our vision and enable us to solve these problems. To this end, some image expressions for quantum computer, such as the flexible representation of quantum images (Le et al., 2011a) and the novel enhanced quantum representation (NEQR) (Zhang et al., 2013), were designed. Quantum image representation plays a key role in quantum image processing. On the basis of these quantum representations, many quantum algorithms have been proposed to process quantum images (Le et al., 2011b; Yao et al., 2017; Iliyasu et al., 2012; Heidari et al., 2017).

Image filtering, which is considered an efficient image processing method, has been widely used for image feature extraction and matching (Singh, 2012; Qian et al., 2019; Zuo et al., 2017). Quantum image filtering has also become the quantum image processing domain active research branch because of its application prospect. The physical quantum convolution of two sequences is impossible because the filter is related to the convolution and correlation in classical image processing (Nielsen and Chuang, 2000). Recently, few papers on the issue of quantum image filtering have been published. In 2013, Caraiman and Manta studied the idea of frequency domain filtering of quantum images. A quantum oracle was used to implement the filter function. The filtering algorithm is effective if the measurement is ignored. The algorithm presents a problem because of the unknown black box of quantum. A spatial filtering approach where the realisation of quantum convolution was avoided, was proposed for quantum images (Yuan et al., 2017a). However, two shortcomings of this method were pointed out, and an improved version was proposed (Yuan et al., 2017b). Unlike the two methods, which mainly focus on mean filtering, the median filtering of quantum images was also investigated (Li et al., 2018; Jiang et al., 2019). The method refers to the quantum median filtering and applications in image de-noising (Li et al., 2018), and the other is an improved quantum image median filtering approach (Jiang et al., 2019). Focusing on the design of the quantum-weighted average filter and its application in image de-noising, Li et al. (2017) provided the quantum circuits that implement the filtering task and presented the results on greyscale images with different noises. Also, they investigated the use of quantum Fourier transform in the field of image filtering for colour images (Li and Xiao, 2018).

Previous works aimed to design the quantum circuits of image filter, reduce computational complexity, and enhance the feasibility of the quantum algorithm. In summary, designing a quantum image filtering scheme is a challenging task.

In this paper, a quantum algorithm for image filtering based on the basic quantum gate operation is proposed. Compared with previous quantum image filtering schemes, the main contributions of this paper are summarised as follows:

1 The quantum image filtering is proposed and implemented by only using small-scale quantum gate operations.

2 All of the reversible logic circuits and the simplified quantum module of the image filter are provided.

3 The proposed quantum algorithm has computational complexity $O(n^2 + 8q^2)$, which is lower than existing quantum filtering schemes.

The article is organised as follows. Section 2 introduces the fundamental concepts in quantum computing and presents the quantum representation of NEQR for image filtering. Section 3 designs four quantum operations by using the basic quantum gates to realise the image filtering algorithm. Section 4 proposes the quantum image filtering algorithm and constructs the corresponding quantum module. Section 5 demonstrates the simulation-based experimental results and computational complexity analyses. Finally, the results are summarised, and conclusions are laid down in Section 6.

2 Preliminaries

2.1 Basic concepts in quantum computation

2.1.1 Qubit

For a quantum computer, information storage and processing are usually in the form of qubits. In a two-dimensional Hilbert space, the qubit $|\varphi\rangle$ can exist as unit vectors, which can be regarded as a general format, that is:

$$|\varphi\rangle = \alpha|0\rangle + \beta|1\rangle \tag{1}$$

where $\alpha, \beta \in C$, $\alpha^2 + \beta^2 = 1$, $\{|0\rangle, |1\rangle\}$ is the computational basis. Generally, for an n qubit system, the computational basis states of this system are of the form $|x_{n-1}x_{n-2}\cdots x_0\rangle$.

2.1.2 Quantum gate

A complex transformation consists of multiple common quantum logic gates (Barenco et al., 1995) in the quantum circuit model. For example, the four quantum gates:

1 NOT gate: This gate is usually used to reverse the contents of the qubit when it acts on. In addition, this gate can be considered a single qubit gate.

2 Hadamard gate: This gate can make 0 and 1 qubits appear with the same probability. In addition, this gate is a single qubit gate.

3 Controlled-NOT (CNOT) gate: This gate is a two-qubit gate that includes the control and target qubits. When the control qubit is 1, the target qubit would be reversed.

4 Toffoli (T) gate: This gate consists of a target qubit, as well as two controls. When both control qubits are 1, the target qubit is flipped.

2.2 NEQR

q qubits are used in the NEQR model to encode colour information. Moreover, $2n$ qubits are used in this model to represent the position information of $2^n \times 2^n$ quantum image, whose greyscale range is $[0, 2^q - 1]$. Equation (2) shows that in the corresponding pixel (Y, X), the binary sequence $C_{YX}^0 C_{YX}^1 \cdots C_{YX}^{q-2} C_{YX}^{q-1}$ can encode the greyscale value $f(Y, X)$ as follows:

$$f(Y, X) = C_{YX}^0 C_{YX}^1 \cdots C_{YX}^{q-2} C_{YX}^{q-1}, C_{YX}^k \in \{0, 1\}, \quad f(Y, X) \in [0, 2^q - 1]. \tag{2}$$

Equation (3) is the expression of a quantum image by using the NEQR model.

$$|I\rangle = \frac{1}{2^n} \sum_{Y=0}^{2^n-1} \sum_{X=0}^{2^n-1} |f(Y, X)\rangle |YX\rangle = \frac{1}{2^n} \sum_{Y=0}^{2^n-1} \sum_{X=0}^{2^n-1} \bigotimes_{i=0}^{q-1} |C_{YX}\rangle |YX\rangle. \tag{3}$$

The position formation is encoded in $|YX\rangle$. The first n-qubit $Y = y_{n-1}y_{n-2}\cdots y_0$ and the second n-qubit $X = x_{n-1}x_{n-2}\cdots x_0$ are used to encode the vertical, as well as the horizontal position formation, accordingly. Figure 1 shows the simple NEQR structure.

Figure 1 NEQR circuit

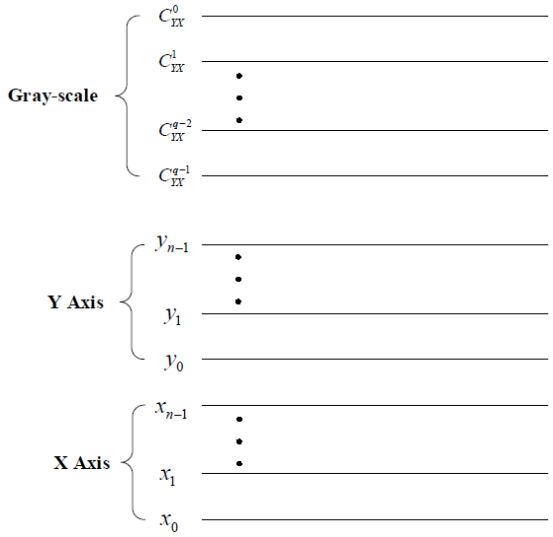

Figure 2 presents a simple quantum image and its expression with four pixels to have a better understanding of this expression.

Figure 2 Sample image and its NEQR expression

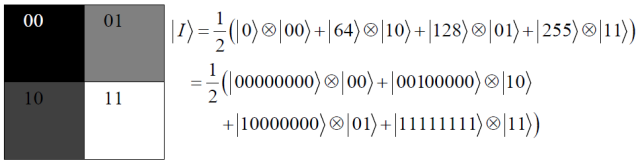

3 Reversible logistic circuit module design

In this section, the following quantum operations are first designed on the basis of some basic quantum gates (in Section 2.1) to realise the quantum filtering algorithm.

3.1 Position shifting operation

The NEQR model maintains the two-dimensional pixel matrix, where the pixel position information and corresponding greyscale value are entangled with each other. Thus, if the entire image is shifted, then each pixel would access the information of its surrounding simultaneously. The idea of cyclic shift transformation was proposed by Le et al. (2011b). On this basis, the entire image can be transformed so that each pixel can access the surrounding information at the same time. To begin with, the definition of a cyclic shift transformation is presented as follows.

Definition: PS($x\pm$) transformation of the NEQR image with size $2^n \times 2^n$ is defined as follows:

$$PS(x\pm)|I\rangle = \frac{1}{2^n} \sum_{Y=0}^{2^n-1} \sum_{X=0}^{2^n-1} |C_{YX}\rangle |Y\rangle |(X \pm 1) \bmod 2^n\rangle. \tag{4}$$

Suppose $X \pm 1$ is replaced with X, then equation (5) can be derived as follows:

$$PS(x\pm)|I\rangle = \frac{1}{2^n} \sum_{Y=0}^{2^n-1} \sum_{X=0}^{2^n-1} |C_{YX'}\rangle |Y\rangle |X\rangle \tag{5}$$

where $X' = (X \text{m} 1) \bmod 2^n$.

For example, if we move one unit of the image to the right, then the pixel has been converted from $f(Y, X)$ into $f(Y, X - 1)$. The specific quantum circuit about cyclic shift transformation of qubit sequence $PS(X-)$ and $PS(X+)$ is shown in Figure 3.

3.2 Parallel-controlled-NOT operation

The bitwise XOR operation of two qubit sequences is accomplished by parallel-controlled-NOT (P-CNOT) operation, and its circuit is illustrated in Figure 4. As shown in P-CNOT module, the first q-qubit sequence is the control qubits, and the second q-qubit sequence is the target qubits.

Figure 3 Position shifting (PS) module, (a) *PS*(*X*+) (b) *PS*(*X*–)

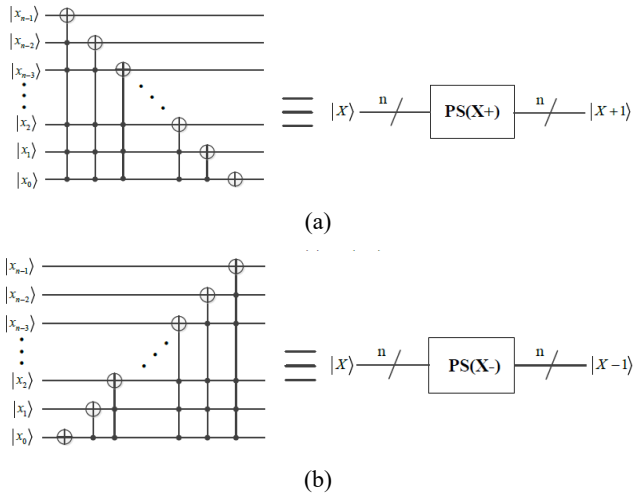

(a)

(b)

Figure 4 P-CNOT module

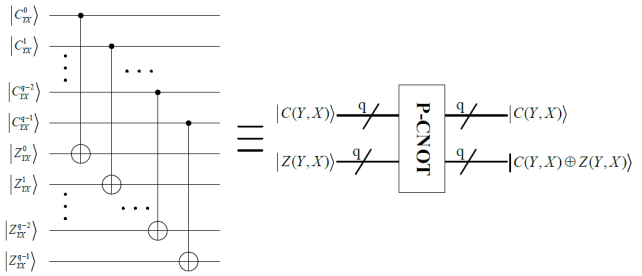

3.3 *Parallel swap operation*

The swap gate can be constructed by three CNOT gates (Figure 5). The swap gate is used to complete the exchange of two qubit states.

Figure 5 Swap gate

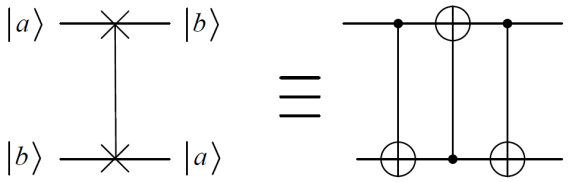

Parallel swap (P-swap) module can be decomposed into q swap gates (Figure 6) by realising the exchange of contents of two qubit sequences (e.g., $|C(Y, X)\rangle$ and $|Z(Y, X)\rangle$).

Figure 6 P-swap modules

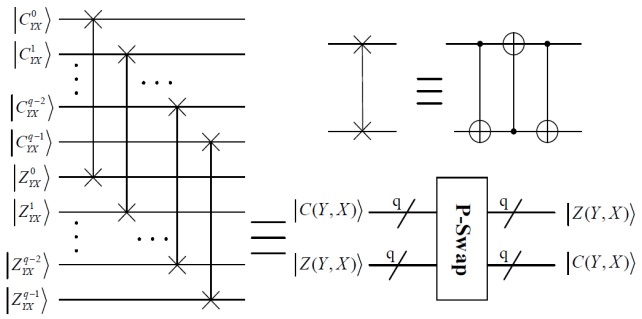

3.4 *Compare the max (Comp-M) operation*

The quantum comparator (Comp) module (Dong et al., 2012) is illustrated in Figure 7. This module is used to compare $|A\rangle = |a_0a_1\cdots a_{q-2}a_{q-1}\rangle$ and $|B\rangle = |b_0b_1\cdots b_{q-2}b_{q-1}\rangle$. The two output qubits $|c_0c_1\rangle$ represent the corresponding comparison result:

- If $|c_1c_0\rangle = |10\rangle$, then $|A\rangle > |B\rangle$.
- If $|c_1c_0\rangle = |01\rangle$, then $|A\rangle < |B\rangle$.
- If $|c_1c_0\rangle = |00\rangle$, then $|A\rangle = |B\rangle$.

Figure 7 Quantum comparator (Comp)

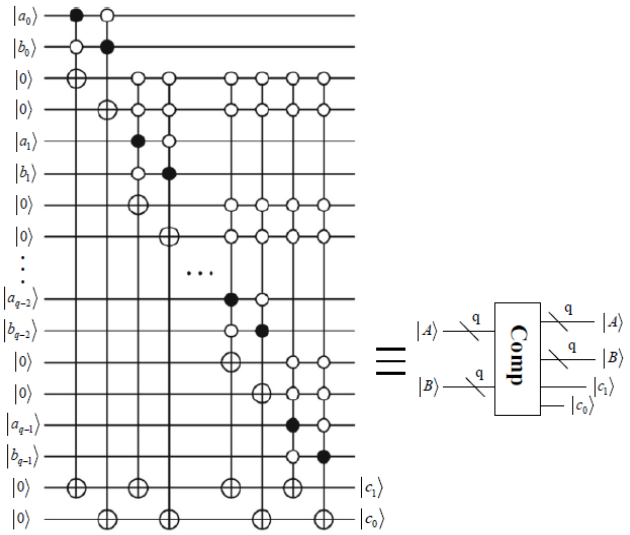

On the basis of the quantum comparator module and P-swap module, we have designed the comparative operation. Figure 8 shows the module of comparing the max operation.

Figure 8 Comp-M module

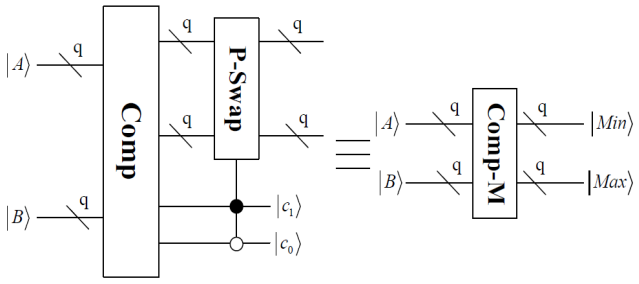

4 Proposed scheme and its quantum circuits

In this section, the classical median filter is first analysed. Then, the workflow of the proposed algorithm is demonstrated. More descriptions of the technical details are also discussed in this section.

4.1 *Median filter*

Median filtering has been widely used in image processing to remove noises. The principle of a filter is to make the

median of the pixels encompassed by the filtering window replace the pixel value of the centre of filtering window. A spatial filter specifically includes an operation that is predefined and a neighbourhood. The operation is executed on the pixels encompassed by the surrounding pixels. A new pixel appears as a result of filtering, whose coordinates are equal to the centre of the neighbourhood coordinates. Then, the filtered image would be generated. Figure 9 shows the feature of spatial median filtering where a 3 × 3 neighbourhood mask is utilised.

Figure 9 Spatial filtering with a 3 × 3 filter mask

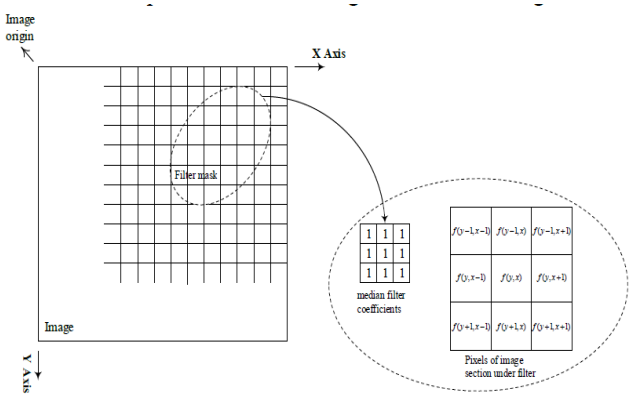

In general, $n \times n$ (n is an odd number) is the common size of the median filter. In general, 3 × 3 filter can meet the filtering requirements in several scenarios. Consequently, the 3 × 3 filter is used to design the quantum image filter in this paper.

4.2 *Quantum circuit realisation of the proposed algorithm*

The original image size is approximately $2^n \times 2^n$, with greyscale range 0, 1, ⋯, $2^q - 1$. By using NEQR, the original image is transformed into quantum image. The extracted pixel is the median value of nine pixels in the 3 × 3 neighbourhood pixels. According to the procedures of classical image median filtering, the whole quantum filtering algorithm framework can be divided into three steps (Figure 10). Detailed descriptions are discussed in this section.

Step 1 PS operations are used to obtain the shifted image set. An empty quantum image set should be prepared as

$$|I\rangle = \frac{1}{2^n}\sum_{Y=0}^{2^n-1}\sum_{X=0}^{2^n-1}|f1(Y,X)\rangle\cdots|f8(Y,X)\rangle|f(Y,X)\rangle|YX\rangle \quad (6)$$

The initial state $|f1(Y,X)\rangle = |f2(Y,X)\rangle = \cdots = |f8(Y,X)\rangle = |0\rangle^{\otimes q}$.

Then, PS and P-CNOT operations should be performed in a certain order. Nine shifted quantum image sets will be generated from the original quantum image $|I_{YX}\rangle$. The shifted quantum image can be defined as

$$\{|I_{Y-1X+1}\rangle, |I_{YX+1}\rangle, |I_{Y+1X+1}\rangle, |I_{Y+1X}\rangle, |I_{Y+1X-1}\rangle \; |I_{YX-1}\rangle, |I_{Y-1X-1}\rangle, |I_{Y-1X}\rangle, |I_{YX}\rangle\} \quad (7)$$

The corresponding reversible logic circuit and its simplified module are designed (Figure 11) to realise the shift operation. The eight shifted images are stored and processed in the specific quantum states. Therefore, the difference between the proposed scheme and the traditional ones is the strategy of image storing and processing. These unique quantum properties, such as superposition and parallelism, can be used to speed up pixel processing.

Step 2 After Step 1, the quantum image set includes 3 × 3 neighbourhood filter mask. The following priority is to find the median value in nine pixels of the 3 × 3 filter mask. As previously introduced and illustrated in Figure 8, the quantum module of Comp-M is used to compare two input qubit sequences. Thereafter, the maximum and minimum values can also be sorted. A simple bubble sort algorithm is executed on the relative images using the Comp-M module to determine the median value of the nine image pixels. Figure 12 illustrates the integrated reversible logic circuit of median filtering 3 × 3 mask and its simplified diagram. In this step, the quantum median filtered image is obtained. The whole quantum system is the entanglement of position qubit sequence. The median filtered pixel qubits are defined in:

$$|I_{MF}\rangle = \frac{1}{2^n}\sum_{Y=0}^{2^n-1}\sum_{X=0}^{2^n-1}|\hat{f}(Y,X)\rangle|YX\rangle. \quad (8)$$

Step 3 Appropriate quantum measurement of the above quantum states is needed to retrieve the median filtered image in the classical form. Figure 13 gives the whole integrate circuit implementation of quantum filtering algorithm. Observing quantum states in a quantum system is difficult because quantum measurements will break the superposition states. Therefore, the construction of the quantum filtered image state needs to be repeated for n ($n \geq 1$) times.

Figure 10 Workflow of quantum filtering algorithm

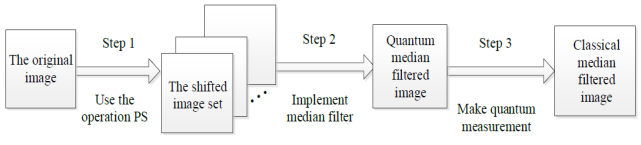

Figure 11 Reversible logic circuit for generating the quantum image set and corresponding quantum module

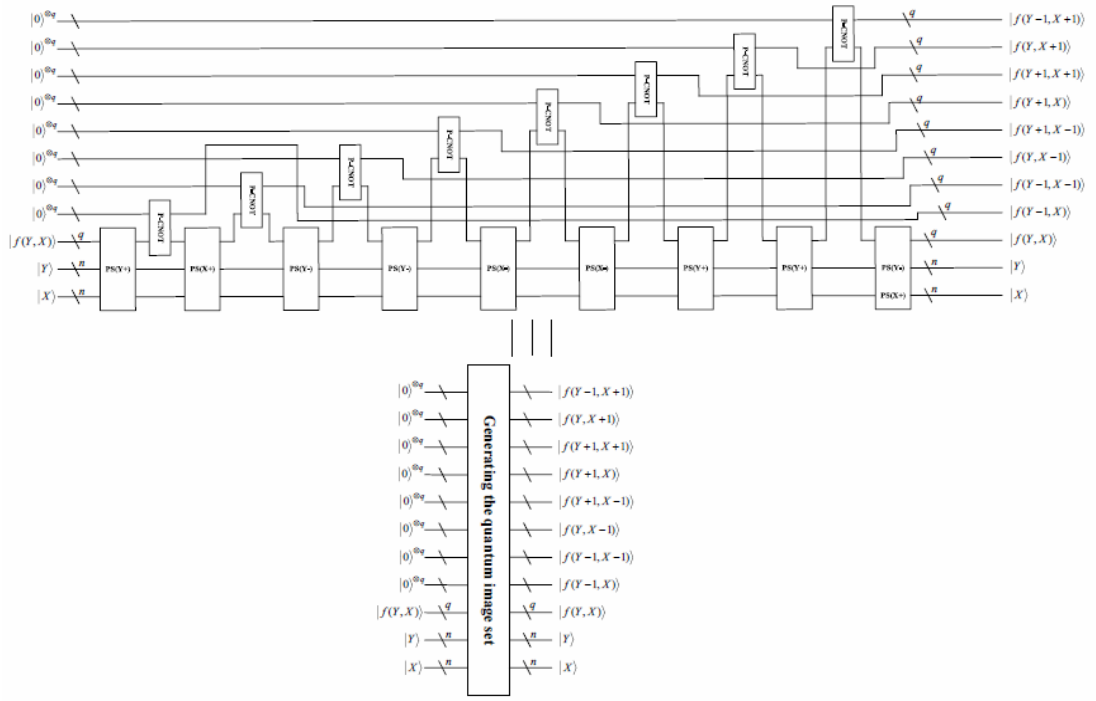

Figure 12 Reversible logic circuit of 3 × 3 median filtering mask and corresponding quantum module

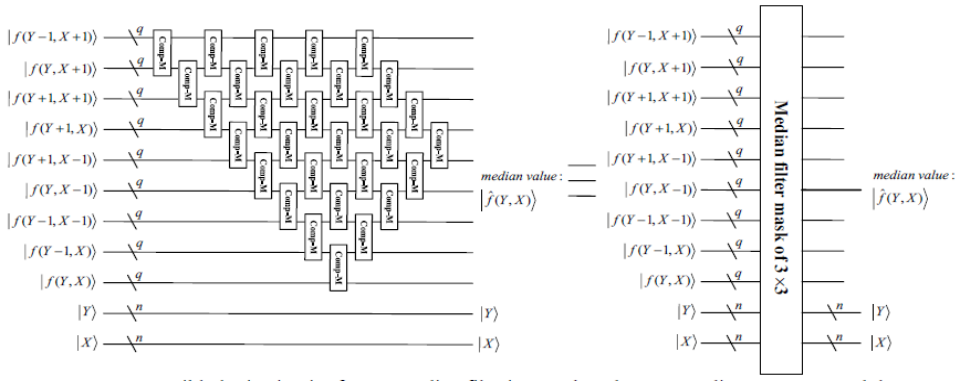

Figure 13 Complete reversible logic circuit of median filtering

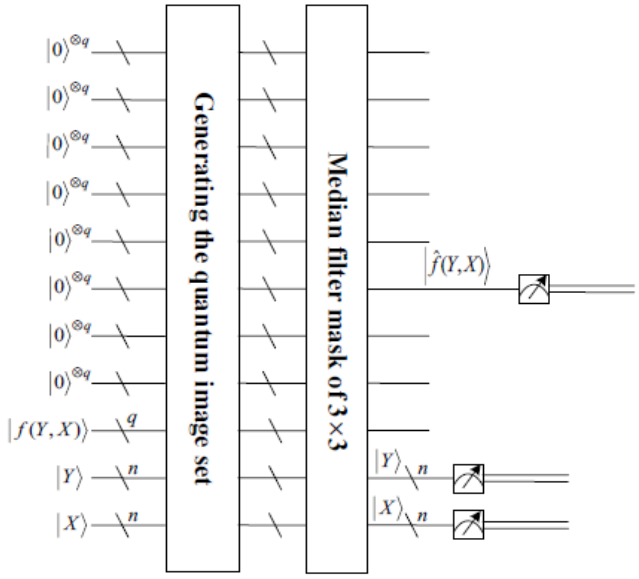

5 Numerical simulations and performance analysis

Considering that a practical quantum computer is unavailable to implement the proposed quantum image filtering scheme, the experiments are limited to classical simulations on a classical laptop using MATLAB R2014b. In the numerical simulation, four greyscale images with size of 512 × 512, namely, Lena, cameraman, pirate and woman, were used as the original image shown in Figure 14.

The simulation procedures are presented as follows. First, salt and pepper noise with densities of 0.20, 0.40, and 0.60 are added to the original images, respectively. After being filtered, the experimental effect is shown in Figure 15. More specifically, Figures 15(a)i–(a)iii, (b)i–(b)iii, (c)i–(c)iii and (d)i–(d)iii show the noise images with densities of 0.20, 0.40 and 0.60, respectively. Figures 15(a)I–(a)III, (b)I–(b)III, (c)I–(c)III and (d)I–(d)III exhibit the corresponding filtered images, respectively. The proposed quantum image filtering could smoothen images

with good effect. Thus, the experimental results indicate that the proposed method can have a good vision that can match the characteristics of human visual system.

Figure 14 Test images, (a) Lena (b) pirate (c) cameraman (d) woman

(a) (b)

(c) (d)

In addition, the histogram is used for further analysis of filtering effect because the same reflects the pixel greyscale distribution of an image. Figures 16(a), (a)i and (a)I show the histograms of original Lena, noise Lena with density 0.2 and filtered Lena, respectively. Figures 16(b), (b)i and (b)I show the histograms of original pirate, noise pirate with density 0.2, and filtered pirate, respectively. Figure 16 show that the histograms of the filtered images are smoother and more uniform than those of the noise images.

5.1 Correlations between adjacent pixels

On the one hand, by randomly selecting 8,000 pairs of adjacent pixels (in horizontal, vertical and diagonal directions) from the original image Lena, noise image Lena with density of 0.2 and filtered image Lena, respectively, the correlation between adjacent pixels are tested. Figure 17 shows the correlation distribution of adjacent pixels in the original, noise and filtered images, respectively. The filtered image also has strong correlation.

On the other hand, the correlation coefficient of the adjacent corresponding images can be calculated. In general, the adjacent pixels' correlation coefficient $R(x, y)$ can be defined as

$$R(x, y) = \frac{E\left(x - E(x)\right) E\left(y - E(y)\right)}{\sqrt{D(x)D(y)}} \tag{9}$$

where $E(x)$ is the expectation of greyscale value, and $D(x)$ represents the variance of the greyscale value.

The correlation coefficient ranges from –1 to 1. The closer the absolute value is to 1, the higher the correlation in an image filtering scheme is. Table 1 shows the correlation coefficients of the adjacent pixels of four different noise images and their corresponding filtered images, respectively. Thus, a, b, c and d are used to represent the original images shown in Figure 14.

Table 1 Correlation coefficients of adjacent pixels for the noise images and their corresponding filtered images

No.	*Different salt and pepper noise densities*			*Corresponding reduction effects under different densities*		
	0.2	*0.4*	*0.6*	*0.2*	*0.4*	*0.6*
a	0.5344	0.3237	0.1869	0.9844	0.8459	0.5272
b	0.5308	0.3217	0.1828	0.9779	0.8369	0.5162
c	0.6212	0.3962	0.2366	0.9902	0.8945	0.6218
d	0.6183	0.3927	0.2325	0.9936	0.9042	0.6213

Table 1 shows that the correlation among adjacent pixels is reduced when imposed with different salt and pepper noise densities. Noise suppression can improve the correlation among adjacent pixels by implementing the filtering algorithm on noise images. The proposed scheme is further proven effective.

5.2 Peak signal-to-noise ratio

Peak signal-to-noise ratio (PSNR) is usually the fidelity index used to compare two monochromatic images, which can be defined as follows:

$$PSNR = 10\log_{10} \frac{\mathrm{MAX}^2}{\sqrt{\frac{1}{2^{2n}} \sum_{i=0}^{2^n-1} \sum_{j=0}^{2^n-1} \left[I_O(i, j) - I_F(i, j)\right]^2}} \tag{10}$$

where I_O is the original image, I_F is the filtered image, and MAX is the maximum value of two images.

The PSNR value (dB) of the noise and filtered images are presented in Table 2, where a, b, c, and d are used to represent the four original images shown in Figure 14. Suppose that P_{i1}, P_{i2}, and P_{i3} denote the PSNR values of the original images and their noise images with densities of 0.2, 0.4 and 0.6, respectively; and P_{f1}, P_{f2}, and P_{f3} denote the PSNR values of original images and their filtered images by using the proposed quantum filtering algorithm. On the basis of the PSNR values depicted in Table 2, the quantum filtering scheme can effectively suppress the impulse noise. Compared with existing quantum filtering schemes (Li et al., 2018; Jiang et al., 2019), experimental results show that the proposed quantum filtering scheme can improve the PSNR of the filtered image even if the same is affected by a higher dense noise.

Figure 15 Noise reduction effect, (a)i–(a)iii, (b)i–(b)iii, (c)i–(c)iii and (d)i–(d)iii are images with salt and pepper noise, (a)I–(a)III, (b)I–(b)III, (c)I–(c)III and (d)I–(d)III are the corresponding filtered results, respectively

Figure 16 Histograms of the original image Lena, noise Lena, and filtered Lena are in (a), (a)i and (a)I, respectively and (b), (b)i and (b)I show the histograms of the original image pirate, noise pirate, and filtered pirate, respectively (see online version for colours)

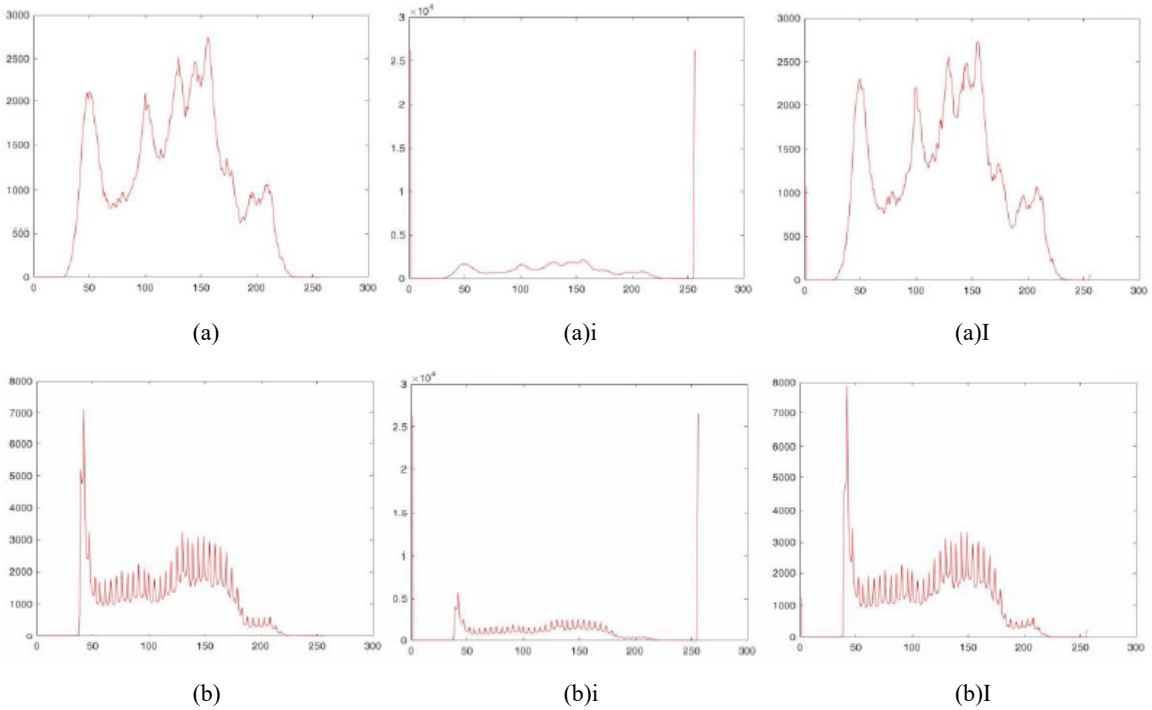

Figure 17 Correlation results, (a), (b) and (c) are the correlation of two horizontally, vertically, and diagonally adjacent pixels in the original image Lena, respectively, (d), (e) and (f) are the correlation of two horizontally, vertically, and diagonally adjacent pixels in the noise image Lena, respectively, and (g), (h) and (i) are the correlation of two horizontally, vertically, and diagonally adjacent pixels in the filtered image Lena, respectively

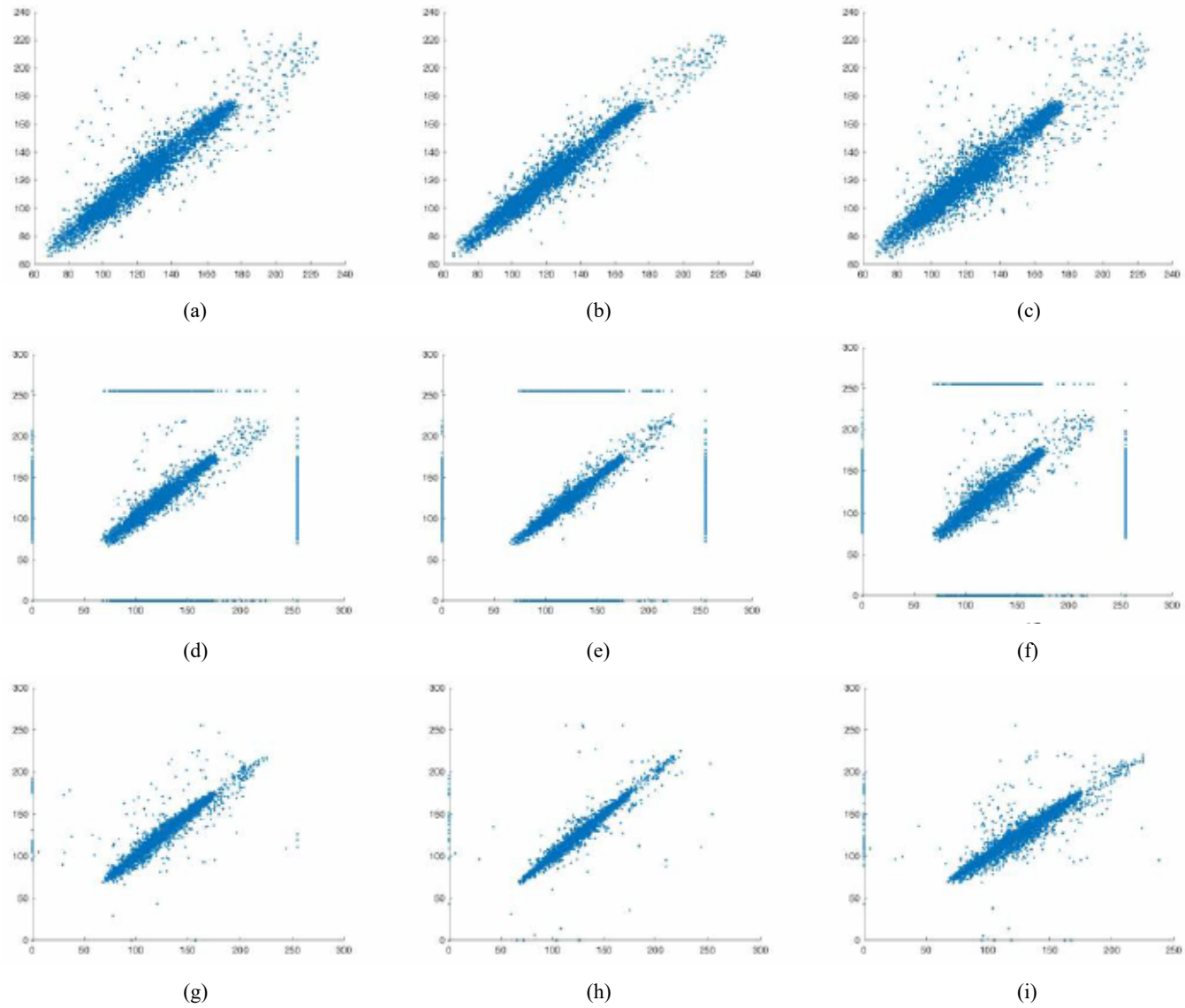

(a) (b) (c)

(d) (e) (f)

(g) (h) (i)

Table 2 Comparison of PSNR (dB)

No.	P_{i1}	P_{i2}	P_{i3}	P_{f1}	P_{f2}	P_{f3}
a	34.0582	31.0412	29.3048	37.3854	35.1823	32.1040
b	34.0583	31.0582	29.2987	35.6441	33.8727	31.4582
c	34.3770	31.4001	29.6366	38.8357	36.0524	32.2216
d	34.0504	31.0276	29.3151	41.5114	37.5023	33.0373

5.3 Computational complexity analysis

In general, a complex transformation in quantum circuit model is composed of several logic gates (Nielsen and Chuang, 2000). In this work, the basic quantum gates are regarded as one. Furthermore, ancillary qubits are used when a complex quantum circuit is designed.

The preparation and measurement of quantum images are often overlooked as part of the quantum algorithm. Thus, the complexity shown in Figure 13 is derived as follows.

The quantum module of generating the quantum image set (Figure 11) includes ten sub-modules of PS and eight sub-modules P-CNOT. The circuit complexity of single PS module is $O(n^2)$, and the P-CNOT module is $O(q)$. Therefore, the complexity is expressed as $O(n^2 + q)$.

The quantum module of the 3 × 3 median filtering mask illustrated in Figure 12 includes 30 sub-modules of Comp-M. The Comp-M module illustrated in Figure 8 is composed of two modules, namely, Comp and P-swap. The q-qubit sequence of Comp module includes the sequence of 2-*CNOT*, ⋯⋯, 2q-*CNOT* gates, and 2q ancillary qubits $|0\rangle$. A k-CNOT gate quantum circuit can be divided into $(4k - 8)$ 2–*CNOT* gate. Thus, complexity can be calculated as follows:

$$\begin{aligned} & 2\times\left(1+\sum_{K=4,6\cdots,2q} 4K-8\right) \\ & =2\times\left(1+8\sum_{K=2,3\cdots,q} K-2\right) \\ & =8q^2-18q+18 \end{aligned} \tag{11}$$

Moreover, the P-swap module shown in Figure 6 can be composed of q Toffoli gates. Its complexity is $O(q)$. Thus, the complexity of the 3 × 3 quantum median filtering mask is approximately $O(8q^2)$.

Through the aforementioned analysis, the complexity of the quantum filtering algorithm (Figure 13) without considering the procedures of preparation and measurement of quantum images is approximately $O(n_2 + 8q^2)$. Apparently, the proposed image filtering algorithm can reduce the computational complexity by using quantum computing. The algorithm is well suited for quantum image filtering. To compare the results of the proposed scheme with those of the previous ones, the presented quantum filtering is compared with Jiang et al.'s algorithm (2019), Yuan et al.'s (2017b) algorithm and Li et al.'s (2018) algorithm, which follow the same spatial filtering method. In Table 3, the proposed scheme outperforms the previous ones in terms of computational complexity.

Table 3 Comparison of computational complexity

Scheme	*Computational complexity*
Jiang et al. (2019)	$O(10n^2 + 21q^2)$
Yuan et al. (2017b)	$O(k^2(n^2 + q^2))$
Li et al. (2018)	$O(28n^2 + 30q^2)$
Proposed scheme	$O(n^2 + 8q^2)$

However, if we consider the case of classical image filtering, the median of all pixels in an image needs to be calculated individually. Thus, for an image with a size of $2^n \times 2^n$, 2^{2n} pixels need to be processed. The computational complexity is $O(2^{2n})$. Consequently, the proposed quantum filtering algorithm can provide exponential speed-up over their classical counterparts.

6 Conclusions

On the basis of NEQR quantum image model, a quantum image filtering scheme combined by using quantum computing and classical median filtering is proposed. Four quantum modules using basic quantum gates are designed to realise the proposed quantum image filtering algorithm. The final reversible logic circuits of quantum algorithm realisation are constructed by these quantum modules. The proposed quantum image filtering scheme has a computational complexity of $O(n^2 + 8q_2)$, which is superior to the existing quantum filtering schemes. Supported by detailed theoretical analysis and simulation, the proposal has also proven its good performance, thereby demonstrating the potential of quantum image filtering for highly efficient image processing in the big data era.

Although our algorithm has some advantages over other algorithms, it also has some shortcomings in terms of colour image filtering. Thus, the proposed algorithm is limited for quantum greyscale image filtering. Future work should focus on the improvement of the proposed algorithm.

Acknowledgements

This work was supported by the Hunan Provincial Natural Science Foundation of China (Grant No. 2020JJ4557) and Research Foundation of Education Bureau of Hunan Province, China (Grant Nos. 18B420 and 19B512).

References

Barenco, A. et al. (1995) 'Elementary gates for quantum computation', *Physics Review A*, Vol. 52, No. 5, pp.3457–3467.

Caraiman, S. and Manta, V.I. (2013) 'Quantum image filtering in the frequency domain', *Advances in Electrical and Computer Engineering*, Vol. 13, No. 3, pp.77–84.

Dong, W., Liu, Z., Zhu, W. and Li, S. (2012) 'Design of quantum comparator based on extended general Toffoli gates with multiple targets', *Computer Science*, in Chinese, Vol. 39, No. 9, pp.302–306.

Feynman, R.P. (1982) 'Simulating physics with computers', *International Journal of Theoretical Physics*, Vol. 21, Nos. 6–7, pp.467–488.

Grover, L.K. (1996) 'A fast quantum mechanical algorithm for database search', in *Proceedings of the 28th Annual ACM Symposium on the Theory of Computing*, ACM, New York, USA, pp.212–219.

Heidari, S., Pourarian, M.R., Gheibi, R., Naseri, M. and Houshmand, M. (2017) 'Quantum red-green-blue image steganography', *International Journal of Quantum Information*, Vol. 15, No. 5, p.1750039.

Iliyasu, A.M., Le, P.Q., Dong, F. and Hirota, K. (2012) 'Watermarking and authentication of quantum images based on restricted geometric transformations', *Information Sciences*, Vol. 186, No. 1, pp.126–149.

Jiang, S., Zhou, R-G., Hu, W. and Li, Y. (2019) 'Improved quantum image median filtering in the spatial domain', *International Journal of Theoretical Physics*, Vol. 58, No. 7, pp.2115–2133.

Le, P.Q., Dong, F. and Hirota, K. (2011a) 'A flexible representation of quantum images for polynomial preparation, image compression, and processing operations', *Quantum Information Processing*, Vol. 10, No. 1, pp.63–84.

Le, P.Q., Iliyasu, A.M., Dong, F. and Hirota, K. (2011b) 'Strategies for designing geometric transformations on quantum images', *Theory Computer Science*, Vol. 412, No. 15, pp.1406–1418.

Li, P. and Xiao, H. (2018) 'An improved filtering method for quantum color image in frequency domain', *International Journal of Theoretical Physics*, Vol. 57, No. 5, pp.258–278.

Li, P., Liu, X. and Xiao, H. (2017) 'Quantum image weighted average filtering in spatial domain', *International Journal of Theoretical Physics*, Vol. 56, No. 11, pp.3690–3716.

Li, P., Liu, X. and Xiao, H. (2018) 'Quantum image median filtering in the spatial domain', *Quantum Information Processing*, Vol. 17, No. 3, p.49.

Nielsen, M.A. and Chuang, I.L. (2000) *Quantum Computation and Quantum Information*, Cambridge University Press, Cambridge, UK.

Qian, J., Zhao, R., Wei, J. et al. (2019) 'Feature extraction method based on point pair hierarchical clustering', *Connection Science*, article in press, DOI: 10.1080/09540091.2019.1674246.

Shor, P.W. (1994) 'Algorithms for quantum computation: discrete logarithms and factoring', in *Proceedings of 35th Annual Symposium on Foundations of Computer Science*, IEEE, Santa Fe, NM, USA, pp.124–134.

Singh, M.K. (2012) 'Vector median filter based on non-causal linear prediction for detection of impulse noise from images', *International Journal of Computational Science and Engineering*, Vol. 7, No. 4, pp.345–355.

Wang, Y. and Vinter, B. (2016) 'Auto-tuning for large-scale image processing by dynamic analysis method on multicore platforms', *International Journal of Embedded Systems*, Vol. 8, No. 4, pp.313–322.

Wang, Y., Wen, H., Jian, Z. et al. (2017) 'A novel WDM-PON based on quantum key distribution FPGA controller', *International Journal of Embedding Systems*, Vol. 9, No. 3, pp.241–249.

Yao, X.W., Wang, H., Liang, Z. et al. (2017) 'Quantum image processing and its application to edge detection: theory and experiment', *Physical Review X*, Vol. 7, No. 3, p.031041.

Yuan, S., Lu, Y., Mao, X., Luo, Y. and Yuan, J. (2017a) 'Improved quantum image filtering in the spatial domain', *International Journal of Theoretical Physics*, Vol. 57, No. 3, pp.804–813.

Yuan, S., Mao, X., Zhou, J. and Wang, X. (2017b) 'Quantum image filtering in the spatial domain', *International Journal of Theoretical Physics*, Vol. 56, No. 8, pp.2495–2511.

Zhang, D., Wang, Q., Wu, X. et al. (2018) 'Unsupervised metric learning for person re-identification by image reranking', *International Journal of Computational Science and Engineering*, Vol. 17, No. 2, pp.159–169.

Zhang, Y., Lu, K., Gao, Y. and Wang, M. (2013) 'NEQR: a novel enhanced quantum representation of digital images', *Quantum Information Processing*, Vol. 12, No. 8, pp.2833–2860.

Zuo, J., Cui, D. and Li, Q. (2017) 'A novel slant transform-based image feature extract algorithm', *International Journal of Embedding Systems*, Vol. 9, No. 3, pp.202–210.